



Title	The Electrical Resistance of Magnesium Under High Pressure
Author(s)	MAEDA, Itaru
Citation	Journal of the Faculty of Science, Hokkaido University. Series 7, Geophysics, 4(3), 81-92
Issue Date	1975-01-31
Doc URL	<a href="http://hdl.handle.net/2115/8880">http://hdl.handle.net/2115/8880</a>
Type	bulletin (article)
File Information	4(3)_p81-92.pdf



[Instructions for use](#)

# The Electrical Resistance of Magnesium Under High Pressure

Itaru MAEDA

(Received Oct. 25, 1974)

## Abstract

Energy bands, the Fermi surface, and the electrical resistance of magnesium as a function of the lattice constants have been calculated by the augmented plane wave method. The calculation shows that electron states in the third Brillouin zone do not disappear but decrease under a compressed state where the electrical resistance shows its maximum. It is also shown that the Fermi surface areas at other lattice constants are nearly the same size. The magnitude of the variation of electrical resistance calculated under certain assumptions is too large to compare with that obtained by Drickamer.

## 1. Introduction

In geophysical studies, the electrical resistance of metals under high pressure is an important quantity. For high pressure experiments the pressure scale is calibrated by the change of electrical resistance of metals. Another example is the investigation of the core state of the earth using the theory of liquid metal.<sup>1)</sup> Carrier for the electrical conduction of the first example is conduction band electrons, and the second example of it is conduction electrons and ions.

The variation of the resistance is a result of that of the electronic structure. It is of great interest to investigate its behavior under high pressure. For this reason, the electrical resistance of magnesium as a function of the lattice constants is investigated by the method of band structure calculation.

For this material, the carriers are the electrons in the conduction band. The crystal structure is hexagonal closed packed (hcp) structure. Because this structure is one of the most dense structure, it is supposed that the material having this structure does not change its form under high pressure. But the axial ratio  $a/c$ , where  $a$  is the length of the  $a$ -axis and  $c$  that of the  $c$ -axis, changes as the crystal is compressed.<sup>2)</sup>

In this paper, the band structures of magnesium at some compressed states

are calculated and the Fermi surfaces are constructed. From these results the variation of the electrical resistance is obtained.

The atomic unit system is used throughout this paper. The energy is measured by Rydberg unit.

## 2. Method of calculation

The band structure calculation is made by the augmented plane wave (APW) method which was offered by Slater in 1937. In this section this method will be explained in some detail. (Further detail is described in the following literatures; Loucks 1967,<sup>3)</sup> Mattheiss et al. 1968<sup>4)</sup>).

In the one electron approximation, the electron system in a crystal is described by

$$H\Psi = E\Psi \quad (1)$$

where  $H = -\nabla^2 + V$  in which the first term is the kinetic energy operator and  $V$  the crystal potential operator.  $\Psi$  is one electron wave function which satisfies the Bloch condition,

$$\Psi_{\mathbf{k}}(\mathbf{r} + \mathbf{R}) = e^{i\mathbf{k} \cdot \mathbf{R}} \Psi_{\mathbf{k}}(\mathbf{r}) \quad (2)$$

where  $\mathbf{R}$  is the direct lattice vector and  $\mathbf{k}$  the wave vector of electron. The crystal potential  $V$  is approximated by the muffin-tin type one which is schematically illustrated in figure 1. In this figure, it is assumed that a potential is spherically symmetric in the region  $AB$  and constant in  $BC$ . This spherically symmetric region is named the APW sphere.

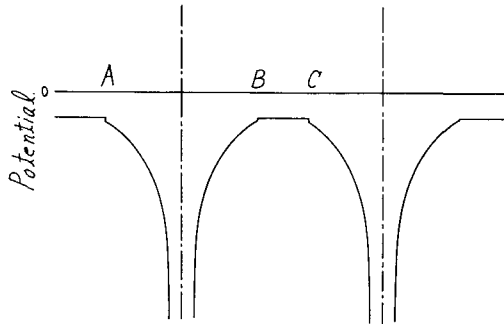


Fig. 1 The illustrative muffin tin potential for one dimensional lattice.

In the APW sphere, the Schrödinger equation (1) is satisfied by a function with a form

$$\psi(\mathbf{r}) = Y_{lm}\left(\frac{\boldsymbol{\rho}}{|\boldsymbol{\rho}|}\right) R_l(\rho) \quad (3)$$

where  $Y_{lm}(x)$  is the spherical harmonics and  $R_l(\rho)$  a function which satisfies

$$-\frac{1}{\rho^2} \frac{d}{d\rho} \left( \rho^2 \frac{dR_l}{d\rho} \right) + \left[ \frac{l(l+1)}{\rho^2} + V_n(\rho) \right] R_l = ER_l \quad (4)$$

In these equations,  $\boldsymbol{\rho}$  is the position vector measured from a center of  $n$ -th sphere,  $l$  the orbital quantum number and suffix  $n$  indicates a potential in the  $n$ -th sphere. In the constant potential region equation (1) is satisfied by a plane wave. Connecting these two types of the function smoothly on the APW sphere surface, the basis functions for the present eigen value problem is obtained, which is called APW and expressed as follows;

$$\phi(\mathbf{k}, \mathbf{r}) = \exp(i\mathbf{k} \cdot \mathbf{r}) \quad \text{for constant potential region.} \quad (5)$$

$$\phi(\mathbf{k}, \mathbf{r}) = 4\pi e^{i\mathbf{k} \cdot \mathbf{r}_n} \sum_{l=0}^{\infty} \sum_{m=-l}^l i^l j_l(kR_{sn}) Y_{lm}^* \left( \frac{\mathbf{k}}{k} \right) Y_{lm} \left( \frac{\boldsymbol{\rho}}{\rho} \right) \frac{R_l(\rho)}{R_l(R_{sn})} \quad (6)$$

for inside the  $n$ -th sphere,

where  $\mathbf{r}_n$  is the position vector of the  $n$ -th lattice point in a unit cell,  $R_{sn}$  the radius of the  $n$ -th APW sphere,  $j_l$  the spherical Bessel function of order  $l$ ,  $i = \sqrt{-1}$  and  $k$  the wave vector.

The variational function  $\Psi$  is a linear combination of the basis functions;

$$\Psi = \sum_i a_i \phi^i \quad (7)$$

where

$$\phi^i = \phi(\mathbf{k} + \mathbf{G}_i) \quad (8)$$

and  $\mathbf{G}_i$  is the  $i$ -th reciprocal lattice vector. The variational expression for the electron energy is as follows;

$$E \int_{\text{unit cell}} \Psi^* \Psi d^3r = \int_{\text{unit cell}} \Psi^* H \Psi d^3r - \frac{1}{2} \int_{\text{sphere}} (\Psi_c^* + \Psi_s^*) \left( \frac{\partial}{\partial \rho} \Psi_c - \frac{\partial}{\partial \rho} \Psi_s \right) dS \quad (9)$$

where suffixes  $s$  and  $c$  indicate the functions for the constant potential region

and for the APW sphere region, respectively. Using

$$\frac{\partial E}{\partial a_i} = 0 \quad i = 1, 2, \dots \quad (10)$$

the secular equation for the present problem is obtained, from which the expansion coefficients  $a_i$  and the electron energy are calculated.

The element of the determinant of the secular equation is expressed as follows;

$$M^{ij} = \Omega(k_j^2 - E) \delta_{ij} - 4\pi \sum_n R_{sn}^2 e^{i(k_j - k_i) \cdot r_n} F_n^{ij} \quad (11)$$

and

$$F_n^{ij} = (k_i \cdot k_j - E) \frac{j_1(|k_j - k_i| R_{sn})}{|k_j - k_i|} - \sum_{l=0}^{\infty} (2l+1) P_l\left(\frac{k_i}{k_i} \cdot \frac{k_j}{k_j}\right) j_l(k_i R_{sn}) j_l(k_j R_{sn}) \frac{R_l'(R_{sn})}{R_l(R_{sn})} \quad (12)$$

The notations are as follows;

$\Omega$  ; unit cell volume

$\delta_{ij}$  ; Kroneker's delta

$j_1$  ; first order spherical Bessel function

$P_l$  ; Legendre function

$k_i = k + G_i$

$k$  ; wave vector in the first Brillouin zone

$$R_l' = \frac{\partial}{\partial \rho} R_l$$

where, bold face letters are vector quantities and the other variables are its norm.

Taking the determinant for equation (11) to be equal to zero, the electron energy is obtained as a function of  $k$ .

The crystal potential is constructed by superposing the free atomic wave functions with electronic configuration  $1s^2 2s^2 2p^6 3s^2$ , using the Herman-Skillman program. The APW sphere radius is taken half the distance of the nearest neighbor. The nine basis functions, i.e. nine reciprocal lattice vectors, are taken which give the energy convergence 0.001 Ryd. The calculated logarithmic derivatives which are the last factor in the right hand side of equation (12) do not have singular points in the energy range of calculation.

The exchange potential is taken as Slater's free electron gas approximation with  $\alpha=1$ . For the value  $\alpha$ , Slater<sup>5)</sup> discussed in great detail.

### 3. The formula for the electrical conductivity

If a electrical field is applied to a system of electrons, the electron states in the reciprocal space shift to the direction of the field. By the collision of electrons to phonons, impurities and the other electrons, the shift becomes a steady state. This shift corresponds to a electric current. If this shift is not so large, the number of electrons corresponding to the shifted states is proportional to the Fermi surface area. Formally this can be expressed as follows (Ziman 1960,<sup>6)</sup> p 268);

$$\sigma = \frac{\tau(k_F)}{4\pi^3} \int v dS \quad (13)$$

where  $\sigma$  : electrical conductivity  
 $v$  : electron velocity in a crystal  
 $dS$ : the Fermi surface element  
 $k_F$ : electron wave number at the Fermi level  
 and  $\tau$  is defined as

$$\tau^{-1} = \int (1 - \cos \theta) L(k, \theta) d\Omega \quad (14)$$

where  $L(k, \theta)$  is the differential transition probability that a particle of momentum  $k$  is scattered through angle  $\theta$  into  $d\Omega$ . Now  $\tau$  is defined by the collision of electrons to phonons or impurities or imperfections of a crystal or the other electrons.

If the electrons are scattered by phonons only, equation (13) can be expressed as follows in the Debye approximation (Ziman,<sup>6)</sup> p 365);

$$\sigma^{-1} = \frac{3\pi \mathcal{A}^6}{4m^* N k \Theta k_F^4 v_F^2} \left(\frac{n}{N_F}\right) \left(\frac{T}{\Theta}\right)^5 D_5\left(\frac{\Theta}{T}\right) \quad (15)$$

where  $n \simeq \int_0^{E_F} N(\epsilon) d\epsilon$

$$\mathcal{A} = (6\pi^2 N)^{1/2}$$

$N$  : the number of scatteres in a unit volume  
 $\Theta$  : the Debye temperature

- $T$  : temperature  
 $m^*$  : effective electron mass  
 $k$  : the Boltzman constant  
 $D_5$  : the Debye integral  
 $N(\epsilon)$ : density of states with energy  $\epsilon$   
 $N_F$  : density of states at the Fermi level  
 $v_F = m^* E_F / K_F$

It is obvious that  $N_F$  is proportional to the Fermi surface area. Then the variation of the electrical conductivity or resistivity can be calculated relatively to a certain reference state as a function of the lattice constants. Because the argument has many limitations, the only rough estimation of the electrical resistance can be done.

### 5. Results and Discussion

The volume ratio, the axial ratio of the  $a$ - and  $c$ -axis at which the electronic structure has been calculated, the inter-sphere constant potential and the Fermi level are shown in the table 1. The Fermi level is measured from the constant potential. At the normal volume  $V_0$ , the lattice constants  $a$  and  $c$  are 6.0569 and 9.8381 atomic unit respectively. Figures 2 to 6 show the band structures at volume ratios 1, 0.85, 0.8, 0.75 and 0.7. The symbols for the symmetrical points are followed from the figure 7 which shows the first Brillouin zone for the hcp structure.

Table 1. The parameters which are used in this study, i.e.  $V/V_0$ ,  $a/a_0$ ,  $c/c_0$ , where  $a_0=6.0569$  and  $c_0=9.8381$  atomic unit. The fourth row indicates the inter-sphere constant potential measured in Rydberg. The Fermi level measured from the constant potential is listed in the last row

$V/V_0$	1	0.85	0.8	0.75	0.7
$a/a_0$	1	0.947	0.927	0.907	0.890
$c/c_0$	1	0.947	0.933	0.912	0.884
Vint	-0.961	-1.095	-1.148	-1.211	-1.282
Ef	0.415	0.501	0.541	0.560	0.620

Energy in rydberg

As a whole the electronic structure is free electron like and do not deform largely relative to each compressed state. The reason why the band shows the almost free electron like structure even at the compressed state may be that, in this study, the non muffin-tin effect has been neglected and the

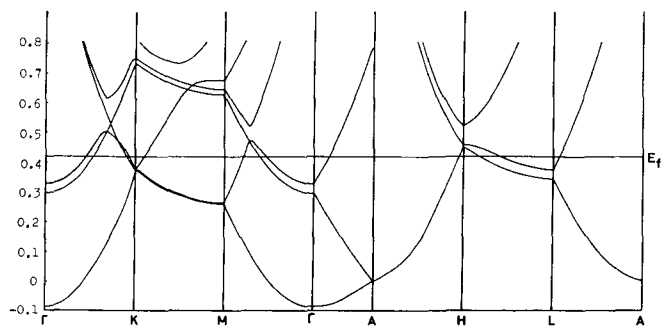


Fig. 2 The band structure of normal state of magnesium along the symmetry lines.

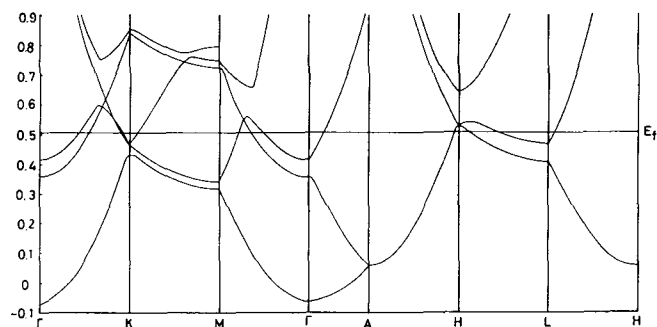


Fig. 3 The band structure of a compressed state corresponding to volume ratio which equals to 0.85.

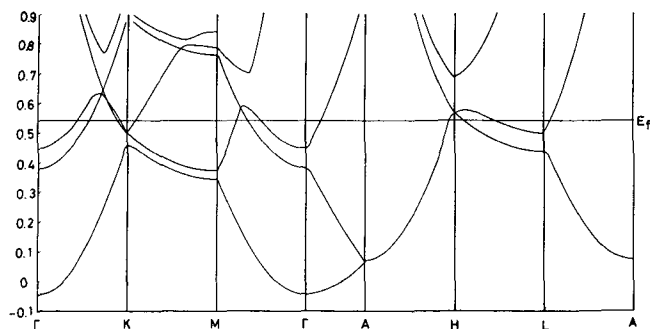


Fig. 4 The band structure corresponding to  $V/V_0=0.8$ .

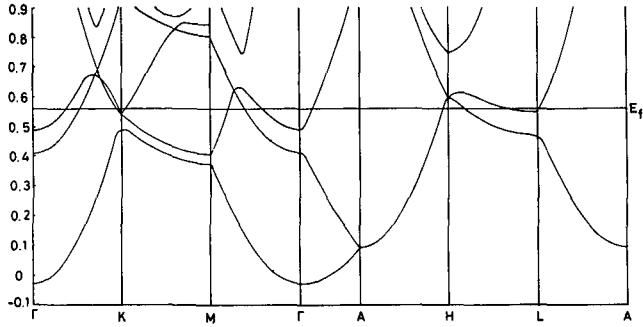


Fig. 5 The band structure corresponding to  $V/V_0=0.75$ . The electrical resistance shows a maximum at this compressed state.

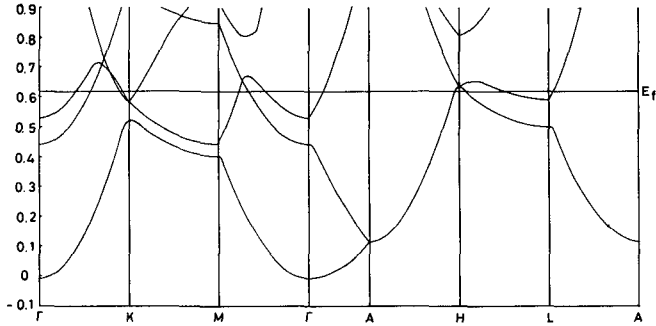


Fig. 6 The band structure corresponding to  $V/V_0=0.7$ . It is seen that the electronic structure almost recovers to that of the normal state.

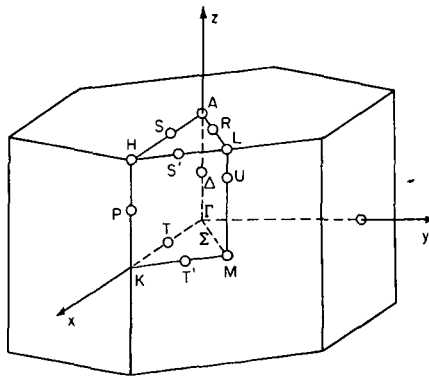


Fig. 7 The first Brillouin zone of the hexagonal closed pack structure. The names of the symmetry points are followed by Koster (1957).

calculations have not been done self-consistently. Although the present calculation has these defects, it is reasonable that the magnesium has the free electron like structure even at compressed state. It is known that the magnesium is simple metal at least at the normal state, and is not subjected to a phase change under high pressure. Then it is expected that the electronic structure is not largely deformed.

The band gap does almost smoothly increase. For example, the variation of it at K-point is shown in table 2. The irregularity is caused by the change of the axial ratio as it is compressed.

Table 2. The band gap between the lowest and the next conduction band at the K-point

$V/V_0$ gap	1	0.85	0.8	0.75	0.7
	0.001	0.042	0.039	0.051	0.060

Energy in Rydberg

The Fermi surface can roughly be deduced from the figures in which the Fermi level  $E_F$  is indicated by a horizontal line. In the one OPW approximation, the Fermi surface can be drawn as the figure 8 in the reduced zone scheme.<sup>7)</sup> The Fermi surface of the third band are drawn in figure 9, in which the broken line indicates the Fermi surface corresponding to the state  $V/V_0=1$ , the bold line corresponding to the state  $V/V_0=0.75$  and the thin

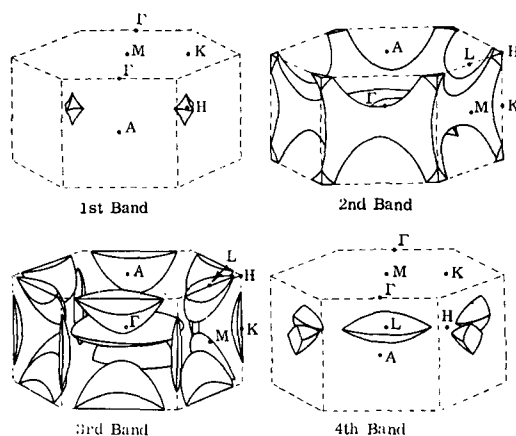


Fig. 8 The one OPW Fermi surface in the reduced zone scheme (after Harrison 1966).

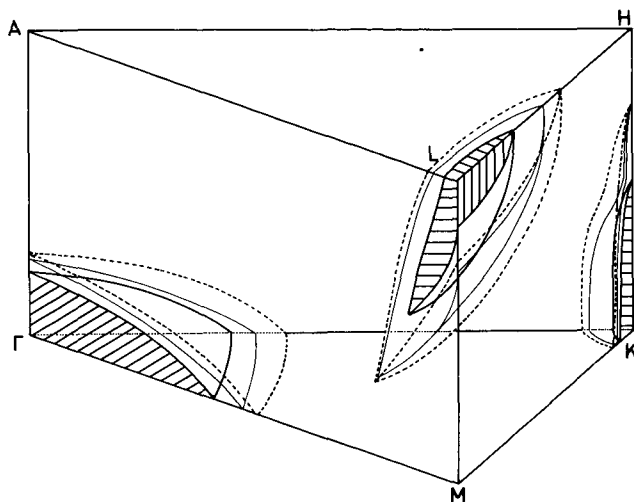


Fig. 9 The calculated Fermi surface in the third zone for the  $1/24$  Brillouin zone. The broken the bold and the thin lines correspond to the state  $V/V_0=1$ , 0.75 and 0.7, respectively.

line corresponding to the state  $V/V_0=0.7$ . For simplicity, they are drawn for the  $1/24$  Brillouin zone. The Fermi surfaces for the other volume are omitted because they are drawn between the broken and thin lines. It follows that the Fermi surface area, i.e. the number of the electron states, decreases but does not disappear at the third band. The collapse of the third band electron states was expected by Drickamer<sup>2)</sup>. Figure 10 shows the experimental resistance and the axial ratio  $a/c$  of magnesium.<sup>2)</sup>

It is found from numerical calculation that equation (15) is not appropriate for a compressed state. Then it is necessary to come back to original equation (13). This equation is so fundamental that many assumptions must be taken for the actual calculation. Assuming that the differential scattering probability is constant, a normalized electrical resistance versus volume ratio is obtained, which is shown in figure 11. The magnitude of the variation of calculated electrical resistance is too large to compare with that obtained by the high pressure experiment. This is caused by the above assumption. Because the number of scatterers increases as a material is compressed, the differential scattering probability also increases. Then it is reasonable that, if the effect of compression on the differential scattering probability is considered, the magnitude decreases. Unfortunately the effect

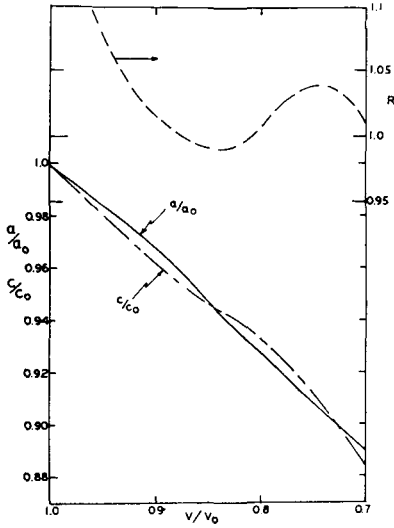


Fig. 10 The variations of  $a/a_0$ ,  $c/c_0$  and the resistance versus  $V/V_0$  for magnesium. (after Drickamer)

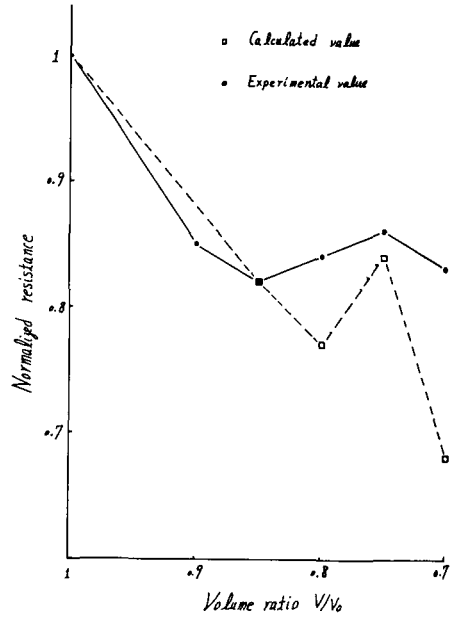


Fig. 11 The calculated and the experimental resistances which are normalized by the values of the normal state. The experimental values are referred from the figure 10.

can not be estimated quantitatively.

### Conclusion

The irregular variation of the electrical resistance of the magnesium is caused by the minor change of the electronic structure which causes a reduction of the Fermi surface area. The change of the electronic structure is caused by the change of the axial ratio of the hcp structure. In this calculations, the axial ratios were given as input data which was reported by Drickamer. Then the cause of the variation of axial ratio was not analyzed. Recently, an experiment in which the axial ratio of magnesium does not vary under high pressure has been reported.<sup>8)</sup> She said that the non hydrostatic pressure effect caused the variation of axial ratio in Drickamer's experiment. But, if this is the case, it can not be understand why only metals having hcp

structure suffer that effect. The axial ratio of hcp structure different from the ideal axial ratio is based on the fact that a potential near the atoms which constitute the crystal is not perfectly spherically symmetric. It is probable that the non spherical part of the potential is easily caused by the effect of the compression.

### References

- 1) EVANS, R. and JAIN, A.: Calculations of electrical transport properties of liquid metals at high pressures, *Phys. Earth Planet. Interiors*, **6** (1972), 141-145.
- 2) DRICKAMER, H.G.: The effects of high pressure on the electronic structure of solids, *Solid State Phys.*, ed. F. Seitz et al., vol **17** (1965), 1-133, Academic Press.
- 3) LOUCKS, T.L.: Augmented Plane Wave Method, (1967), 256 pp Benjamin.
- 4) MATTHEISS, L.F., WOOD, H.J. and SWITENDICK, A.C.: A procedure for calculating electronic energy bands using symmetrized augmented plane waves, *Methods in Comput. Phys.*, ed. Alder et al., vol **8** (1968), 63-147, Academic Press.
- 5) SLATER, J.C.: *Quantum Theory of Molecules and Solids*, vol 4 (1974), 583 pp McGraw Hill.
- 6) ZIMAN, J.M.: *Electrons and Phonons*, (1960), 554 pp Oxford.
- 7) HARRISON, W.A.: *Pseudopotentials in the Theory of Metals*, (1966), 336pp Benjamin.
- 8) SATO, Y. (1974) private communication.